JOURNAL OF GEOPHYSICAL RESEARCH, VOL. 104, NO. C6, PAGES 13,479–13,488, JUNE 15, 1999

Wavenumber-frequency structure of infragravity swash motions

K. T. Holland

Naval Research Laboratory, Stennis Space Center, Mississippi

R. A. Holman

College of Oceanic and Atmospheric Sciences, Oregon State University, Corvallis

Abstract. Alongshore-separated time series of natural swash motions were obtained over a range of environmental conditions using a video technique. Although the frequency spectra and normalized wavenumber spectra for these motions were particularly bland, wavenumber-frequency spectra of these data showed clear partitions of infragravity band energy levels associated with various wave types. For the frequencies $0.025 < f \leq 0.05$ Hz, 45 ± 13% of the shoreline variance was, on average, associated with high-mode ($n \geq 2$) edge waves and/or leaky waves, while approximately half that amount was associated with low-mode edge waves. Gravity wave motions (comprising both edge and leaky modes) were typically dominant in a lower-frequency band ($0.001 < f \leq 0.025$ Hz). A substantial portion of the variance in this band (21 ± 10%, with a maximum of 38%), however, was identified as a nondispersive waveform with wavenumbers well outside of the wavenumber-frequency bounds for gravity waves. Surprisingly, this nongravity swash variance showed no significant dependence on mean alongshore current strength or mean alongshore current shear as measured in the surf zone trough separating the shoreline from an offshore bar. In addition, the celerities of these swash zone nondispersive waves were found to differ in magnitude, and in one instance, sign, from celerities of similarly structured waves measured farther offshore in the surf zone. These unexpected observations with respect to low-frequency, nongravity swash energy imply a strong decorrelation between trough and shoreline fluid motions.

1. Introduction

1.1. Background

Using laboratory observations, *Miche* [1951] suggested that swash motions due to monochromatic waves can be saturated, in that shoreline oscillations are limited in magnitude by a constant that depends on wave frequency and beach slope. For random waves, the expectation is that an increase in wave energy above this threshold results in an increase in wave dissipation offshore. Frequency components that are not dissipated in the surf zone and survive to be reflected at the shoreline will correspondingly be those waves of relative low frequency and have been loosely termed infragravity energy. Extensive field evidence supports this expectation, in that energy at infragravity frequencies often constitutes a large portion of the total energy observed at the shoreline during storms [*Suhayda*, 1974; *Huntley*, 1976; *Holman*, 1981; *Guza and Thornton*, 1982; *Holman and Sallenger*, 1985; *Raubenheimer and Guza*, 1996].

In addition to being an important component of shoreline motions, energy within this infragravity frequency band (nominally 0.004 - 0.05 Hz) has been hypothesized to influence nearshore morphology such as sand bar generation and beach cusp development (see reviews by *Holman and Sallenger* [1993] and *Inman and Guza* [1982], respectively). In both cases, the bar position or cusp spacing can be theoretically tied to a specific wave frequency f or longshore wavenumber k. More complicated structures could be explained by the interaction between multiple waves of equal frequency with differing discrete wavenumbers [*Bowen and Inman*, 1971; *Holman and Bowen*, 1982]. Therefore the specific frequency and wavenumber characteristics of wave motions within the infragravity band are of interest because of this potential coupling between nearshore hydrodynamic and morphologic structures.

In this paper, we present results using a video technique to characterize the frequency and wavenumber structure of swash on a barred beach. We found that infragravity swash motions are broad banded in frequency and generally concentrated around low wavenumbers, although, occasionally, energetic motions at relatively high wavenumbers were detected outside of the frequency-wavenumber bounds of gravity waves. Relationships to various environmental parameters and analogous offshore measurements were also tested in an attempt to parameterize the temporal variation in swash structure and to determine the cause of the nongravity motions.

1.2. Theory and Previous Observations

Theoretical relationships between radial frequency ($\omega = 2\pi f$) and radial alongshore wavenumber ($\kappa = 2\pi k$) exist following *Eckart* [1951]. He found analytic solutions to the linear, shallow-water equations of motion for free gravity waves to be

$$\Phi(x,y,t) = \frac{ag}{\omega}\phi(x)\cos(\kappa y - \omega t + \theta) \qquad (1)$$

where Φ is the velocity potential, x is the cross-shore coordinate, y is the alongshore coordinate, a is the wave amplitude at the shoreline, and $\phi(x)$ is a frequency or wavenumber dependent cross-shore nodal structure. For $|\kappa| < \omega^2/g$, waves form a contin-

Paper number 1999JC900075.
0148-0227/99/1999JC900075$09 00

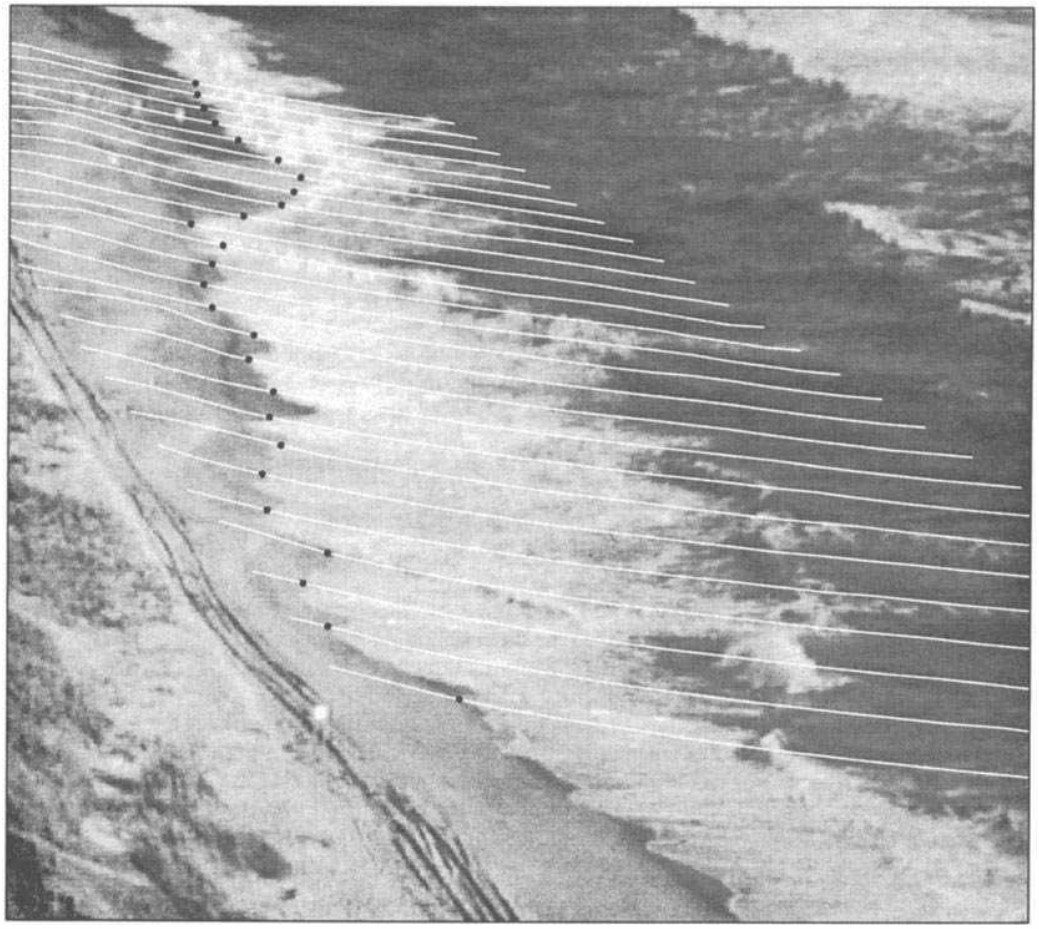

Figure 1. Video image from the DELILAH experiment showing alongshore-separated, cross-shore transects at which swash elevation measurements were made. Swash edge locations as identified by computer are signified by circles. The total alongshore coverage is 250 m.

uum in f-k space, called leaky waves, whose energy is not constrained to the nearshore. For $\omega^2/g \le |\kappa| \le \omega^2/g\beta$, a series of discrete modes called edge waves exist such that for planar beaches of slope β

$$\omega^2 = g\kappa\sin[(2n+1)\beta]; \quad n = 0,1\ldots, \quad (2n+1)\beta < \frac{\pi}{2} \tag{2}$$

[*Ursell*, 1952]. For $|\kappa| > \omega^2/g\beta$, no gravity wave solutions exist. The form of the above solutions for gravity wave motions suggest that wavenumber may be normalized to yield $\kappa' = \kappa/(\omega^2/g)$ and that the free wave domain may be split by

$$|\kappa'| < 1 \tag{3a}$$

for leaky waves,

$$1 \le |\kappa'| \le 1/\beta \tag{3b}$$

for edge wave modes,

$$|\kappa'| > 1/\beta \tag{3c}$$

for nongravity waves. In addition, bound wave motions resulting from the forced displacement of the free water surface by the structure of wave groups [*Longuet-Higgins and Stewart*, 1964] are possible and have no theoretical dependence on κ.

Using these dependencies, the variance of infragravity band fluid motions can be divided into specific energy partitions associated with leaky waves, edge wave modes, bound waves, and nongravity waves. For example, several researchers have demonstrated that infragravity wave motions in the swash and surf zones are often dominated by cross-shore standing waves that are strongly reflected at the shoreline (equivalent to leaky waves) [*Suhayda*, 1974; *Huntley et al.*, 1981; *Guza and Thornton*, 1985; *Holland et al.*, 1995; *Raubenheimer et al.*, 1995; *Raubenheimer and Guza*, 1996]. Edge wave modes have also been convincingly shown to be a contributing factor to infragravity fluid motions in the surf zone [*Huntley et al.*, 1981; *Oltman-Shay and Guza*, 1987; *Howd et al.*, 1991]. In addition, a nondispersive waveform known as a shear wave, that has potential vorticity rather than gravity acting as a restoring force, has been identified in surf zone measurements within the infragravity frequency band [*Oltman-Shay et al.*, 1989]. Finally, bound waves have been found to contribute to infragravity wave energy [*Guza et al.*, 1984; *Elgar and Guza*, 1985; *Okihiro et al.*, 1992].

2. Methods

Swash data were collected during the DELILAH experiment, conducted at the U. S. Army Corps of Engineer's Field Research Facility in Duck, North Carolina, from October 4 - 19, 1990 [*Birkemeier et al.*, 1997]. Video recordings of swash were made using a camera mounted 43 m above mean sea level and positioned looking alongshore. Swash elevation time series were

sampled at 1 Hz from these recordings along 26 cross-shore transects spaced every 10 m in the longshore (Figure 1). Following digitization of individual video frames, the intensities of image pixels along surveyed beach profile transects were searched to find the most landward pixel location exceeding a time-averaged threshold intensity. The survey elevation corresponding with that pixel is defined as the runup value R for that transect at that instant in time. The vertical resolution of this technique, estimated by mapping the horizontal resolution to an elevation along the profile, varies as a function of distance from the camera but was typically less than 3 cm. Total run durations varied between 1.5 and 2 hours. An example of swash time series collected using this method is given in Figure 2.

Swash frequency spectra $E(f)$, wavenumber spectra $E(k)$, and wavenumber-frequency spectra $E(k, f)$, were computed from 1024 point ensembles (with 50% overlap) that were individually detrended to remove tides and tapered with a Kaiser-Bessel window. A frequency bin width of 0.002 Hz was chosen and resulted in between 20 and 28 degrees of freedom. $E(k, f)$ spectra were estimated at infragravity wave frequencies using the iterative maximum likelihood estimator (IMLE) developed by *Pawka* [1982, 1983]. A cyclic wavenumber bin width of 0.0005 m^{-1} was selected. The cross-spectral matrix for the IMLE incorporated time series from alongshore locations lagged by up to 120 m (the approximate maximum distance over which motions were coherent in the infragravity band). Multiple sets of nonoverlapping time series measurements were treated as spatial ensembles to produce an averaged cross-spectral matrix. Quantitative comparison of the IMLE spectra with lower spatial resolution spectra computed using a two-dimensional fast Fourier transform showed consistent energy peak levels.

Complementary data collected by other investigators included bidirectional current meter data from alongshore arrays (along the nearshore bar and trough, respectively) and one cross-shore array, tide elevations outside the surf zone, and daily nearshore bathymetry data. Also, incident band wave statistics were calculated from bottom pressures sampled in 8-m depth.

Tide, current, and wind wave climatology along with other associated parameters are displayed in Figure 3 and show the range of conditions experienced in this study. A period of low-energy swell was interrupted by the passage of a frontal system on October 10, resulting in maximum significant wave heights H of up to 2 m and strong alongshore currents V to the north (up to 1.4 m/s). Even higher waves, 2.3 m, arrived in association with Hurricane Lili on October 13 as narrow-banded swell with a relatively small angle of incidence α. Following October 15, seas were mixed with two periods of current reversal resulting in flow to the south. The average tidal range over the period of the experiment was approximately 1.5 m. Wave periods T ranged between 5 and 15 s. The alongshore-averaged foreshore slope β (defined as the best fit linear slope within the region between the maximum runup and minimum rundown) varied over the experiment between 0.06 and 0.11 (with a mean standard deviation over the array length of 0.014). Alongshore-averaged significant swash height averaged 1.9 m and Iribarren values, $\xi_0 = \beta/(H_s/L_0)^{0.5}$, during the experiment ranged from 0.4 to 1.5.

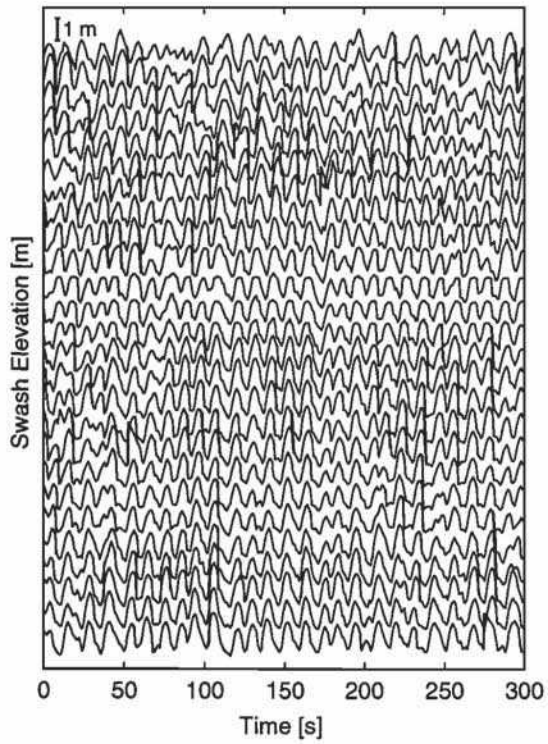

Figure 2. Sample 5-min segment of swash elevation time series from the October 15, 1990, 1141 LT data run. The 26 adjacent transects are offset with distance north increasing up the page. Evident is an incident wave periodicity of approximately 13 s. The alongshore coherence of the wave motion lends confidence in the digitization process. A 1-m vertical scale is also shown.

3. Observations

Of 65 possible data runs, 26 runs spanning a variety of environmental conditions were selected for analysis. The remaining runs (39) had to be excluded owing to difficulties in digitization including poor lighting conditions, extreme low tides causing the shoreline along some transects to fall outside of the camera view, and/or the presence of animals, humans or vehicles obstructing clear view of the beach transects.

3.1. Frequency Spectra

Figure 4a shows frequency spectra for multiple transects for a typical run. These spectra are well approximated by their alongshore-averaged spectrum $\overline{E}(f)$ (Figure 4b), which shows several obvious characteristics. For the incident wave frequency band ($f > 0.05$ Hz) there is a dominant peak in energy at 0.07 Hz (a lower frequency than the offshore incident wave peak) and an approximately f^{-4} decay in energy at frequencies above 0.1 Hz. This decay pattern (the high-frequency roll-off in energy) mimics that found by *Guza and Thornton* [1982] and *Huntley et al.* [1977] using field data from a different beach and is consistent with this portion of the spectrum being saturated. In contrast, infragravity energy spectra (which were modeled in terms of a $\log_{10}(\overline{E}) = mf + b$ form) showed a basically flat spectral slope, which was rarely red (Figure 4b), implying that the infragravity portion of the swash spectrum is typically unsaturated. Maximum and minimum values of the best fit linear spectral slope ranged between -6.8 and 8.1. Note that an order of magnitude change in energy within the infragravity band would have an m value of 20.

The data were also examined for the presence of statistically significant spectral peaks, which might serve as indicators of large amplitude, spatially coherent, periodic signals. Only two of

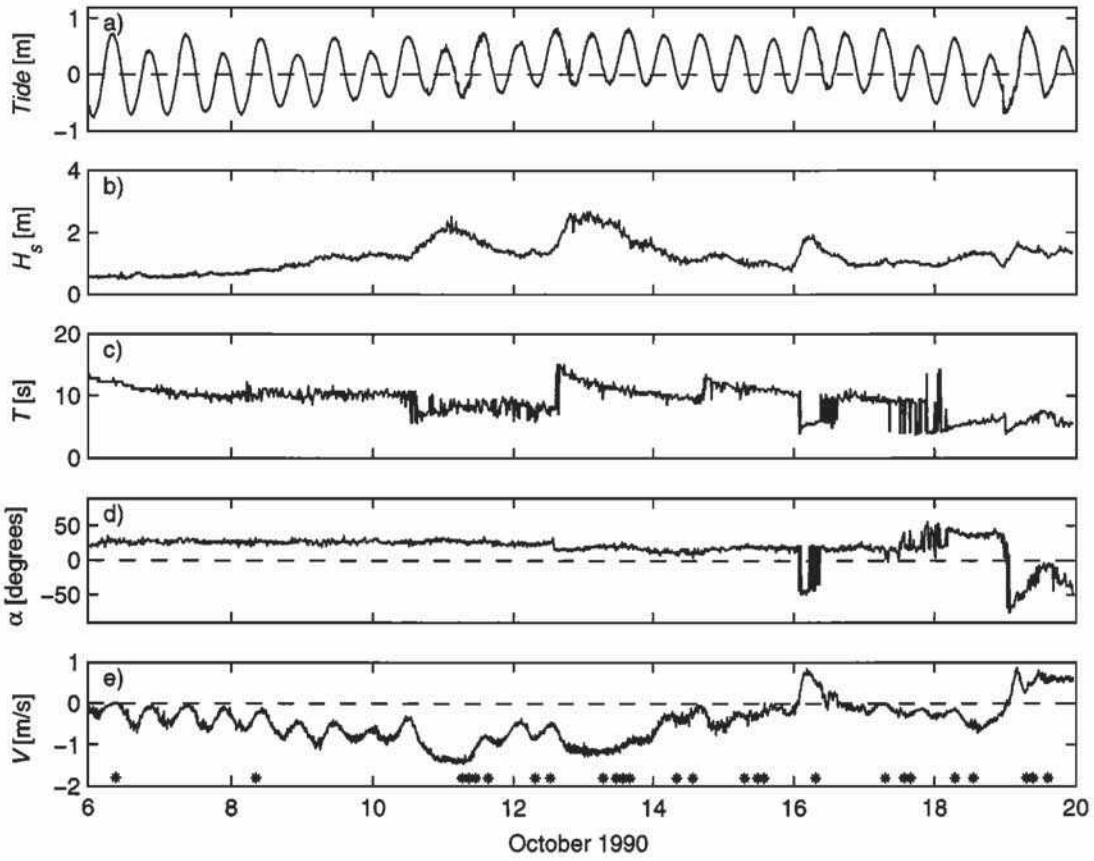

Figure 3. Temporal variations in (a) tide level, (b) significant wave height, (c) wave period, and (d) incidence angle measured in 8-m depth and (e) alongshore current speed measured in the trough of the offshore bar during the DELILAH experiment. Asterisks indicate timing of the swash data runs.

the 26 alongshore averaged spectra (8%) had peak values (defined as a spectral density estimate greater than the two adjacent estimates) larger than the linear spectral slope (explained above) plus a 95% confidence interval. Additionally, only 7% of the individual swash spectra showed energy levels inconsistent with the null hypothesis that the infragravity signals are equivalent to white noise [following *Percival and Walden*, 1993]. Therefore there was little evidence of significant peaks in the infragravity band of these data.

Significant coherence over the length of the array was commonly observed in the incident frequency band, especially at the incident peak frequency. Within the infragravity band, average longshore coherence length scales (i.e., the length scale over which wavenumber-integrated motions were significantly coherent for a particular frequency) were of the order of 100 m or slightly less than half the array length. Maximum and average (over frequency) infragravity band length scale values were 196 and 51 m, respectively.

3.2. Nondimensional Wavenumber Spectra

In an effort to determine whether dominant peaks were present in the wavenumber space of the swash motions, dimensionless wavenumber spectra $\bar{E}(\kappa')$ were calculated over the range $|\kappa'| \leq 20$ (where $\kappa' = \kappa/(\omega^2/g)$) by integrating across the frequency band 0.025 - 0.05 Hz. This interval was selected to exclude nongravity wave energy (previously defined as $|\kappa'| > 1/\beta$) and to assure that wavenumber resolution was sufficient to separate leaky and high-mode edge wave energy from that of low modes (defined in this paper to be $n < 2$). The spectra were computed using the dimensional spectral density values obtained by applying the IMLE estimator over a consistent region in κ' space. Changes in variance over frequency were smoothed by applying the estimator to a normalized cross-spectral matrix (unit diagonal elements) with total power within individual frequency bins normalized to 1. This restriction allowed consistent (over frequency) energy peaks at specific nondimensional wavenumbers κ' to be emphasized.

Figure 5 shows a typical, dimensionless wavenumber spectrum. The bulk of the energy is concentrated at small wavenumbers with a half-power width well outside the region of low-mode edge waves. The lack of visible high-wavenumber peaks does not indicate that no such peaks were present, just that low-mode structure was not consistently apparent over multiple frequencies.

To summarize the findings over all runs, we chose to describe the characteristic shape of these normalized wavenumber spectra in terms of a best fit Gaussian form defined by

$$\tilde{E}(\kappa') = A\exp[\frac{-(\kappa'-\kappa'_0)^2}{2\sigma^2_{\kappa'}}] + nf \tag{4}$$

where A is a peak amplitude, κ'_0 is a wavenumber offset, $\sigma_{\kappa'}$ is a

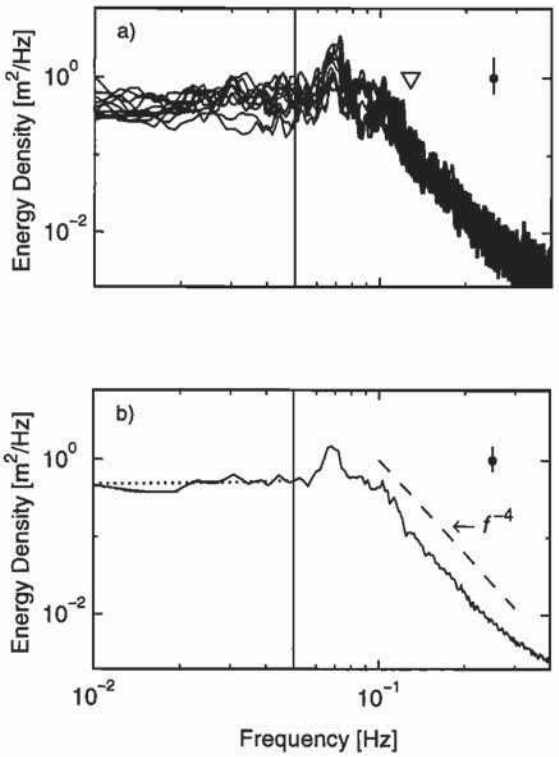

Figure 4. (a) Energy density spectra of swash elevation for run on October 17, 1338 LT, corresponding to each of the 26 alongshore transects. The 95% confidence interval is shown. Inverted triangle indicates the peak frequency of deepwater waves, and the solid line represents the cutoff frequency (0.05 Hz) separating incident and infragravity bands. (b) Average frequency spectrum over the 26 transects. A confidence interval corresponding to 56 degrees of freedom is shown assuming a decorrelation length scale of the order of half the array length. The dotted line indicates a best fit slope (see text) to the infragravity portion of the spectrum, and the dashed line represents the f^{-4} saturation dependence proposed by *Huntley et al.* [1977].

wavenumber standard deviation, and *nf* is a noise floor. The nonlinear model parameters were obtained using a Levenberg-Marquardt algorithm [*Press et al.*, 1992]. The results indicate that the fit does a good job of characterizing the single-peaked, low-wavenumber, gravity wave structure within the high/leaky mode partition. The average (over the runs) correlation coefficient r^2 between the curve fit and the observations was 0.98. The minimum correlation was 0.93, and all runs were visually inspected to verify the absence of strong secondary peaks. The average root-mean-square error describing the mismatch between $\overline{E}(\kappa')$ and $\tilde{E}(\kappa')$ was 0.0006.

One interesting observation concerning the normalized wavenumber spectra is that the wavenumber offset κ'_0 typically was not zero (the mean value was –0.67). This suggests that unequal amounts of high-mode/leaky wave energy were commonly propagating in opposite directions. A strong correlation ($r = 0.74$) was observed between κ'_0 and incident swell propagation directions, and only two of the 26 runs had upcoast or downcoast propagation directions opposite to that of the incident waves. These correlations support similar findings by *Herbers et al.* [1995a] for infragravity waves on this same beach, but in 13-m depth.

3.3. Wavenumber-Frequency Spectra

Although the one-dimensional descriptions given by the frequency spectra and wavenumber spectra presented in sections 3.1 and 3.2 are useful as indicators of the bulk characteristics of infragravity shoreline motions, the overall wavenumber-frequency spectrum was used to determine the relative contributions of various wave energy types to shoreline variance. For an alongshore homogeneous and temporally stationary wave field, wave energy associated with edge or leaky waves would be expected to lie along ridges in wavenumber-frequency space, according to dispersion relationships such as (2) (but modified for topographic and current effects following *Howd et al.* [1992] and *Oltman-Shay and Howd* [1993]). Energy resulting from forced waves would be broadly distributed.

A sample infragravity band *k-f* spectrum computed using the iterative maximum likelihood estimator is shown in Figure 6. Dispersion lines for mode 0 and mode 1 edge waves and the leaky mode cutoff are indicated. Several features are obvious. Foremost, there is a large amount of energy at low wavenumbers, suggestive of leaky or high-mode ($n \geq 2$) edge waves (and consistent with the results in section 3.2). A linear ridge at far

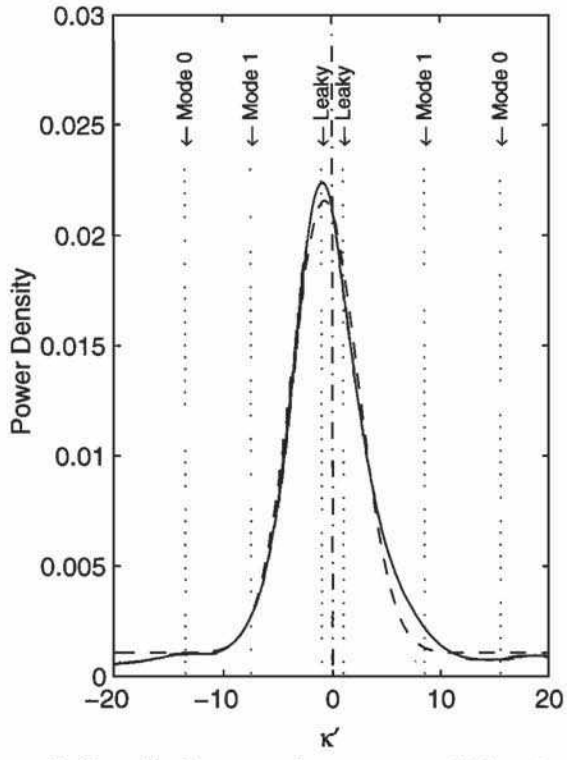

Figure 5. Normalized wavenumber spectrum (solid line) for run on October 17, 1338 LT over the frequency band $0.025 < f \leq 0.05$ Hz. Nondimensional (see text) low-mode edge wave and leaky mode cutoff wavenumbers are indicated by the dotted lines and were calculated for the measured topography and mean alongshore currents. Dashed line indicates the best fit to the Gaussian form. The r^2 correlation coefficient between the observed and fitted spectra is 0.99, and the root-mean-square (rms) error is 0.0072.

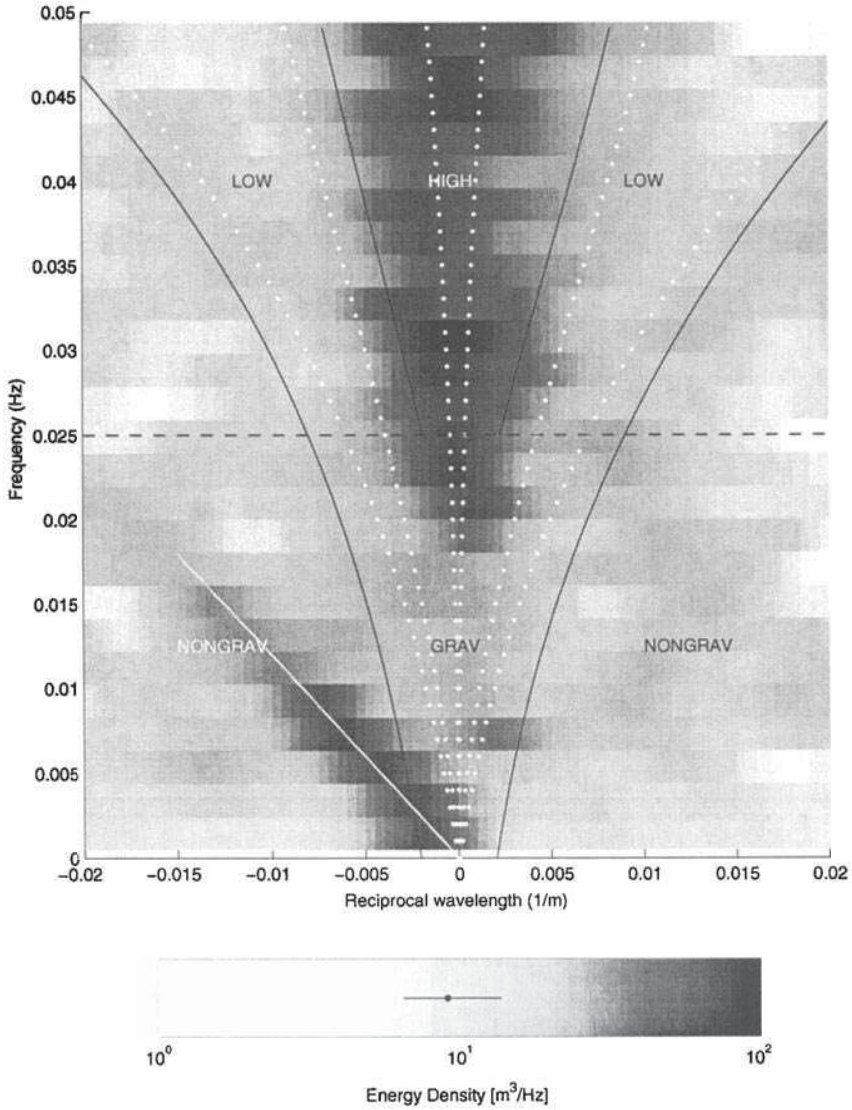

Figure 6. The iterative maximum likelihood estimator (IMLE) based wavenumber-frequency spectrum of swash elevation for the October 17, 1990, 1338 LT data run. Shading intensity represents energy density levels displayed on a log scale (gray scale ban shown). Dotted lines indicate the dispersion curves for mode 0 and mode 1 edge waves and the leaky wave cutoff for measured bathymetry and currents along a cross-shore transect in the approximate center of the video array. Dark solid lines indicate the variance partitions bounding the HIGH, LOW, GRAV, and NONGRAV wave types (the variance levels within each partition relative to the total variance within the infragravity band are 29, 9, 16, and 17%, respectively). The light solid line represents a best fit linear trend to the nongravity energy ridge. A 95% confidence interval for energy density is specified within the gray scale bar.

infragravity band frequencies ($0.001 < f \leq 0.025$ Hz) is also apparent in the wavenumber region outside the bounds for gravity waves and corresponding to the region where shear wave energy would be expected. There are few suggestions of energy being concentrated along the dispersion curves for low-mode edge waves.

Although this example is illustrative of the general forms of the observed *k-f* spectra, the individual spectra varied significantly between the 26 runs. To summarize these data, variance was partitioned within four wavenumber-frequency regions corresponding separately to low-mode edge waves (LOW), high-mode and/or leaky waves (HIGH), very low frequency gravity waves (GRAV), and very low frequency nongravity wave type motions (NONGRAV). (The wavenumber resolution was insufficient to distinguish confidently between high-mode and low-mode edge waves at low frequencies < 0.025 Hz, hence the generic GRAV partition.) The partitions were defined as follows

$$\sigma^2_{\mathrm{GRAV}} = \int_{0.001}^{f_c} \int_{-k_0(f)-\delta}^{+k_0(f)+\delta} E(k,f)\,dk\,df$$

$$\sigma^2_{\mathrm{NONGRAV}} = \int_{0.001}^{f_c} \int_{-k_M}^{+k_M} E(k,f)\,dk\,df - \sigma^2_{\mathrm{GRAV}}$$

$$\sigma^2_{\mathrm{HIGH}} = \int_{f_c}^{0.05} \int_{-k_1(f)+\delta}^{+k_1(f)-\delta} E(k,f)\,dk\,df$$

$$\sigma^2_{\mathrm{LOW}} = \int_{f_c}^{0.05} \int_{-k_0(f)-\delta}^{+k_0(f)+\delta} E(k,f)\,dk\,df - \sigma^2_{\mathrm{HIGH}} \qquad (5)$$

where σ^2 is the integrated variance in each of the partitions; $\pm k_0(f)$ and $\pm k_1(f)$ are the estimated mode 0 and mode 1 edge wave

Table 1. Measured Variance σ^2 Within Each Partition and Percent Variance

	Mean	Standard Deviation	Maximum	Minimum
$\sigma^2_{NONGRAV}$	0.0051	0.0041	0.0188	0 0008
σ^2_{GRAV}	0.0121	0.0078	0 0294	0 0028
σ^2_{LOW}	0.0065	0.0050	0.0212	0.0009
σ^2_{HIGH}	0.0138	0.0093	0 0337	0 0022
σ^2_{igbot}	0.0264	0.0164	0.0730	0.0084
σ^2_{igtop}	0.0307	0.0209	0 0873	0.0072
%NONGRAV	21.2	10.0	38 1	3 3
%GRAV	44 7	12.5	72.2	27.1
%LOW	20.8	6.4	30 3	8.1
%HIGH	45 0	13.0	70 6	25.6

Values are in m^2. Subscripts are defined as follows: NONGRAV, very low frequency nongravity wave type motions; GRAV, very low frequency gravity waves; LOW, low-mode edge waves; HIGH, high-mode and/or leaky waves; igbot, variable with bottom half of infragravity band; and igtop, variance within top half of infragravity band. Variance percentages are calculated as 100 times the ratio of the measured variance normalized by the variance within either the top or bottom infragravity frequency band, whichever was appropriate.

wavenumbers, respectively, as a function of frequency; $\pm k_M$ are the maximum and minimum wavenumber bounds; and δ is a constant wavenumber offset (0.002 m^{-1}) to account for discrete wavenumber bandwidth of the spectral peaks. The frequency band cutoff f_c was defined to be 0.025 Hz to separate the top and bottom halves of the infragravity band (no obvious nongravity wave energy was observed at frequencies greater than 0.025 Hz), and k_M was set to 0.05 m^{-1} (the Nyquist wavenumber of the array).

To separate broadband energy levels from significant peaks associated with edge, leaky, and nongravity waves, a uniform noise floor was defined following the two-step process suggested by *Oltman-Shay and Guza* [1987]. A mean energy density level was determined from all peaks in the frequency-wavenumber spectrum within the infragravity band. A second, low mean energy level was calculated for energy beneath the first level. The noise floor was then determined as the low peak mean level plus its standard deviation. We assumed that peaks beneath this noise floor cannot be confidently regarded as having a frequency-wavenumber dependence and therefore set energy levels beneath this critical threshold to zero. Changes in calculated variance due to different noise floor definitions (mean versus median) were typically less than 5%.

Observed variance levels within each of the four partitions relative to the variance within the infragravity band are given in Table 1. Mean values (plus or minus 1 standard deviation) over the experiment for σ^2_{HIGH} and σ^2_{LOW} were 138 ± 93 cm^2 and 65 ± 50 cm^2, respectively, compared with a mean total variance for frequencies $0.025 < f \leq 0.05$ Hz of 307 ± 209 cm^2. Mean values for σ^2_{GRAV} and $\sigma^2_{NONGRAV}$ were 121 ± 78 cm^2 and 51 ± 41 cm^2, compared with a mean total variance for frequencies $0.001 < f \leq 0.025$ Hz of 264 ± 164 cm^2. These mean values relative to the total variance within the infragravity frequency band correspond to percentages of 24, 11, 21, and 10% for the HIGH, LOW, GRAV, and NONGRAV partitions, respectively. Partitioned variances levels over time are given in Figure 7.

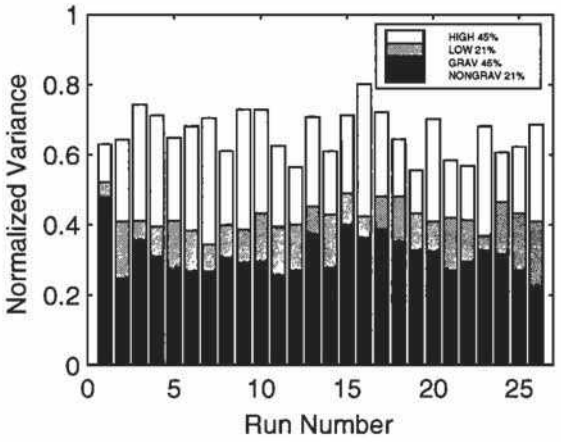

Figure 7. Variance contributions within the four partitions relative to the total variance within the infragravity band. Wave type partitions are identified in the key (top right), with average percentage contributions shown relative to the variance level within the frequency interval (top or bottom) of each partition.

These quantities indicate that, on average, 56 ±6% of the infragravity band shoreline variance could be attributed to energy peaks in the *k-f* spectra associated gravity waves (of either edge or leaky wave types) and 10 ±6% to nongravity waveforms. The remainder of the variance (34%) was either beneath the noise floor cutoff value or outside the gravity wave bounds in the upper

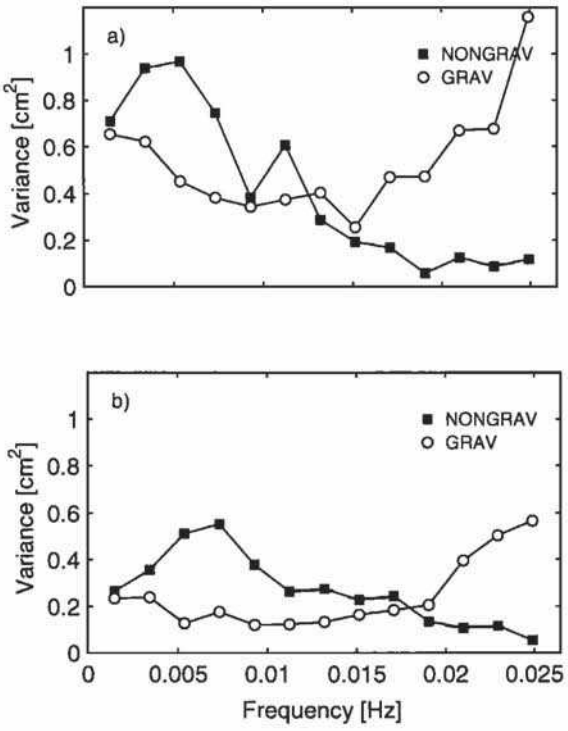

Figure 8. Variance in the GRAV (circles) and NONGRAV (squares) wave partitions as a function of frequency for runs (a) October 16, 0728 LT, and (b) October 17, 1338 LT. Nongravity wave variance generally increases with decreasing frequency. At some frequencies, nongravity wave variance exceeds gravity wave variance by as much as a factor of 3.

frequency partition and roughly constrained the maximum amount of broadband energy that could be associated with bound waves. At higher infragravity frequencies ($0.025 < f \leq 0.05$ Hz), the amount of high/leaky mode energy commonly exceeded that of low-mode edge waves, in many cases, by more than a factor of 2. This result is consistent with the single low-wavenumber peak observed in the normalized wavenumber spectra. On average (over frequency and runs), in the bottom half of the infragravity frequency band ($0.001 < f \leq 0.025$ Hz), shoreline variance within the GRAV partition was approximately twice that of the NONGRAV partition.

Interestingly, for the few runs where nongravity waves were obvious (e.g., Figure 6), variance within the nongravity wave partition did occasionally equal or exceed the gravity wave variance level at particular frequencies. For example, Figure 8 shows this nongravity wave dominance as a function of frequency for two runs. These observations suggest that for a limited number of cases the contribution of nongravity motions to infragravity shoreline variance can be significant.

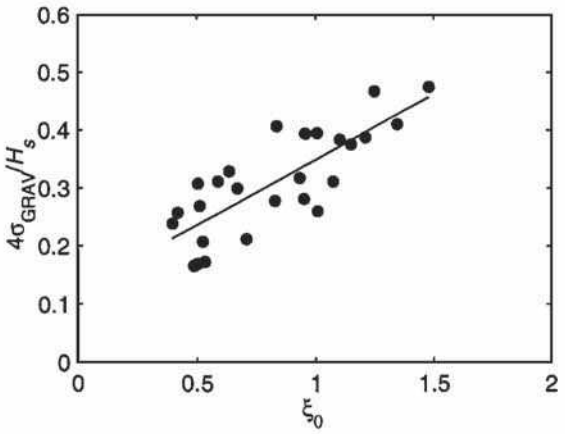

Figure 9. Shoreline variance within the GRAV partition converted to significant swash height and normalized by significant wave height as a function of Iribarren number, ξ_0. Slope (intercept) coefficients for the fit are 0.22±0.07 (0.12±0.06). The fit explains 64% of the observed variance.

3.4. Environmental Dependencies

The range of conditions experienced during DELILAH allowed daily fluctuations in swash elevation variance within the wave type partitions to be correlated against measured offshore wind wave variance, tidal levels, and other environmental parameters (Table 2). Swash variances within the GRAV, LOW, and HIGH partitions were found to be significantly correlated to offshore wave energy as given by H_s. The fact that gravity wave variance levels (i.e., exclusive of the nongravity wave category) increased with increasing offshore incident wave height in 8-m depth suggests that these motions are unsaturated. In addition, a roughly linear relationship between swash variance in these partitions and swell energy in 8-m depth was observed, suggesting that these are free motions because bound wave energy would be expected to increase quadratically with swell energy. This observation of free wave dominance in infragravity motions supports the findings of *Elgar et al.* [1992] for offshore energy measurements at the same site.

The lack of observed correlation between the measured variance within the NONGRAV partition and incident wave energy is not surprising since the *k-f* structure of this energy suggests a nongravity waveform similar to shear instability [*Bowen and Holman*, 1989]. However, it is extremely surprising that no significant correlations were observed between NONGRAV variance and the hypothesized forcing for shear waves as represented by either the observed cross-shore shear of the mean alongshore current (averaged over the run) or the absolute value of the measured mean alongshore current. In fact, NONGRAV is the only partition to show insignificant correlations with $|\overline{V}|$ or $d\overline{V}/dx$. (The significant correlations between variance in the other partitions (GRAV, LOW, and HIGH) and these alongshore current parameters closely mimic the corresponding correlations with significant wave height and most likely reflects the condition of moderate correlation between currents and waves.)

Table 2. Correlation Matrix of Variance Versus Environmental Parameters

	$\overline{R}$	Tide	β	T	H_s	$\lvert\overline{V}\rvert$	$d\overline{V}/dx$
$\sigma^2_{NONGRAV}$	(0.63)	(0.59)	(0.62)	0.09	0.03	-0.05	0.14
σ^2_{GRAV}	0.38	0.18	(0.44)	(0.47)	(0.74)	(0.67)	(0.66)
σ^2_{LOW}	(0.74)	(0.56)	(0.68)	0 31	(0.53)	(0.43)	(0.47)
σ^2_{HIGH}	0.31	0 09	0.32	(0.39)	(0.77)	(0 73)	(0.65)

Variables are defined as follows: $\overline{R}$, runup value; β, beach slope; T, wave period; H_s, significant wave height; $|\overline{V}|$, absolute value of mean alongshore current; $d\overline{V}/dx$, cross-shore shear of the mean alongshore current. Correlations r significantly different from 0 with 95 (99)% confidence have absolute values greater than 0.39 (0.50) and are shown in parenthesis. Variance values were calculated over the frequency intervals corresponding to the partitioned variance levels. No significant correlations were observed with either incidence angle α or Iribarren number ξ_0.

In addition, the *k-f* structure of the NONGRAV energy at the shoreline was often markedly different from that observed farther offshore. Nongravity wave celerities were computed as the best fit linear trend in *k-f* space to energy ridges within the NONGRAV wave partition for the swash measurements and for temporally consistent velocity measurements sampled in the trough of the offshore bar approximately 75 m seaward of the shoreline. Of the 11 runs where linear slopes could be detected in the offshore spectra, three of the runs had similar celerities (to within 10 cm/s) while five runs had no linear feature apparent in the swash. Two of the remaining runs had swash celerities that were roughly twice that observed offshore, and in one case, on October 16, the sign of the celerity of nongravity waves in the swash was opposite to that measured in the trough. The percentage of variance in the NONGRAV partition relative to the total variance in the $0.001 < f \leq 0.025$ Hz frequency band for these 11 runs was also much greater offshore, up to 85%, compared with a maximum of 38% for measurements obtained in the swash zone.

Significant correlations were also found between the LOW and NONGRAV variance levels and environmental parameters representative of specific beach characteristics, namely, the mean foreshore slope and certain mean water level values such as tide height and the mean swash level (Table 2). The signs of the correlation coefficients indicate that energy in these partitions increased as the water level rose and the beach became steeper. Given that Duck is a concave barred beach, the beach steepness and near-to-shore wave heights would be expected to increase with higher water levels; however, the fact that this sensitivity was mainly reflected in only the LOW and NONGRAV partitions

is important. A linkage to specific physical forcing is implied such as the possibility that at higher tides, strong longshore currents are generated near the shoreline, which may influence shear wave or low-mode edge wave generation in the swash.

Even though none of the partitioned variance levels showed a direct dependence on deepwater Iribarren number, when converted to significant heights and normalized by incident wave heights (as in Figure 9), significant linear trends of moderate skill were found for each partition (explaining, on average, 44% of the observed variance). This Iribarren dependence supports the findings of *Holman and Sallenger* [1985] for this same location that nonpartitioned infragravity band oscillations are larger under dissipative conditions than under reflective conditions for a given offshore height.

4. Discussion

Our observations from the DELILAH experiment show that a substantial portion of the shoreline variance within the infragravity band (on average, 56%) was associated with unsaturated, free gravity waves. This result is similar to findings by previous researchers for infragravity band currents and sea surface elevations measured farther offshore [*Suhayda*, 1974; *Holman*, 1981; *Huntley et al.*, 1981; *Oltman-Shay and Guza*, 1987; *Herbers et al.*, 1995b]. The remainder of the energy was either due to broadband energy, including potentially forced motions, or to waves that are not governed by gravity as a restoring force.

Although a number of researchers have presented the relative contributions of edge, leaky, and bound wave energy in the surf zone and nearshore (most recently, *Elgar et al.* [1989], *Howd et al.* [1991], and *Okihiro et al.* [1992]), the only prior wave type partitioning of shoreline variance is that of *Oltman-Shay and Guza* [1987]. These authors estimated that low-mode edge waves dominated longshore velocity measurements in the surf zone and contributed as much as 50% of the energy at the shoreline during their experiment. However, the Oltman-Shay and Guza energy computations were based on the extrapolation of nearshore current amplitudes to the shoreline using analytical theory; no wavenumber-frequency spectra were computed using direct measurements of alongshore-separated swash motions. For comparison, our data suggest an average swash zone, low-mode contribution of the order of only 21%, with a maximum of 30%. Since the low-mode definition of these authors ($n \leq 2$) was less restrictive than the definition used in this study ($n < 2$) and the analysis methods differed, it is possible and consistent that the contribution of low modes to shoreline variance is often significant. However, on the basis of our more direct observations, the two lowest edge wave modes are rarely dominant energy sources relative to high modes and leaky waves in the swash zone.

Perhaps more intriguing is the observation of nongravity wave motions at the shoreline. The energy distribution in k-f space of these signals closely mimics the characteristics of shear waves previously observed farther offshore at the same site [*Oltman-Shay et al.*, 1989]. Shear waves are assumed to have a sea surface elevation signal that is small compared with horizontal fluxes [*Bowen and Holman*, 1989] and therefore were presumed to have no influence on the shoreline swash elevation signal. *Holman et al.* [1990] found no indication of shear wave expression in the swash over four data runs (even under conditions when shear wave energy was evident in velocity data taken 50 m offshore) and used this observation as confirmation of this rigid lid assumption. However, our observations apparently contradict both the presumption of a shoreline rigid lid and prior findings.

Interestingly, we found a lack of correlation between nongravity wave variances and the observed alongshore current structure, the hypothesized forcing mechanism. This discrepancy suggests that swash zone nongravity waves are not directly driven by the shear of offshore currents. This suggestion seems to be confirmed by the markedly different celerities observed at the shoreline and farther offshore. Observations of unequal celerities at two distinct cross-shore locations imply that different waves or at least different forcing mechanisms are present. One possible explanation is that the nondispersive swash waves are driven by a shoreline jet of longshore-directed flow that may differ in direction and magnitude from that of the alongshore current observed in the bar trough offshore. Although this speculation is unproven since the most landward current meter installation during DELILAH was more than 25 m from shore, numerical modeling of alongshore velocities near the shoreline has shown similar oscillation patterns [*Kobayashi and Karjadi*, 1996].

Regardless of the forcing mechanism, the identification of the nongravity shoreline signals is important. The swash elevation variance associated with the NONGRAV wave partition occasionally equaled or exceeded the variance due to gravity waves within the same frequency band, particularly at very low frequencies (less than 0.017 Hz in Figure 8). This dominance is intriguing since most previous studies of swash zone motions have ignored the possibility of nongravity waveforms. *Holland et al.* [1995] found that at very low infragravity frequencies ($0.001 < f < 0.02$ Hz), swash amplitude measurements exceeded that expected for linear gravity waves (including low modes), but they were unable to determine the cause of the overamplification. *Raubenheimer and Guza* [1994] showed similar findings using a nonlinear model. The present results suggest one possible source for the unexplained variance would be the presence of nongravity wave energy similar to that measured during DELILAH that would not have been modeled by either the linear or nonlinear gravity wave theory. Unfortunately, alongshore wavenumber spectra could not be calculated from the *Holland et al.* [1995] results, and therefore this possibility was not confirmed. Clearly, further field and theoretical studies are needed to verify whether the nongravity wave observations in the swash zone can be modeled as shear wave instabilities.

5. Summary

Twenty-six sets of swash time series sampled over a 250-m alongshore array and collected over a range of environmental conditions have been used to establish the wavenumber and frequency structure of infragravity band shoreline motions. Typical frequency spectra in the infragravity band had little energy structure, and wavenumber spectra were dominated by energy at low wavenumbers. Variance partitioned over wavenumber and frequency indicated that more than 50% of the infragravity band swash variance was associated with wavenumber peaks within the gravity wave region (including both edge and leaky wave types). The remainder of the energy was either broad-banded, showing no coherent frequency-wavenumber relationship, or was identified (at approximately 10% of the total infragravity variance) as being a nondispersive, nongravity waveform found to be unrelated to both the magnitude and shear of the alongshore current measured in the surf zone. This finding suggests that surf and swash zone motions may be decoupled.

Acknowledgments. This research was supported by base funding from the Office of Naval Research (ONR) to NRL, the ONR Coastal

Dynamics Program, and the U.S. Geological Survey, National Coastal Geology Program. Special thanks go to Michael Freilich and to the two anonymous reviewers for their helpful and instructive comments

References

Birkemeier, W A., C. Donoghue, C.E. Long, K.K. Hathaway, and C.F. Baron, 1990 DELILAH Nearshore Experiment: Summary report, *Tech. Rep. CHL-97-24*, 213 pp., U.S. Army Corps of Eng. Waterw. Exp. Stn., Vicksburg, 1997.

Bowen, A.J., and R.A. Holman, Shear instabilities of the mean longshore current, 1, Theory, *J. Geophys. Res.*, *94*(C12), 18,023-18,030, 1989.

Bowen, A.J., and D.L. Inman, Edge waves and crescentic bars, *J. Geophys. Res.*, *76*(36), 8662-8671, 1971.

Eckart, C., Surface waves on water of variable depth, *Wave Rep. 100. Ref. 51-12*, 99 pp., Scripps Inst. of Oceanogr., La Jolla, Calif., 1951.

Elgar, S., and R.T. Guza, Observations of bispectra of shoaling surface gravity waves, *J. Fluid Mech.*, *161*, 425-448, 1985.

Elgar, S., J. Oltman-Shay, and P. Howd, Observations of infragravity-frequency long waves, 1, Coupling to wind waves, *Eos Trans. AGU*, *70*, 1333, 1989.

Elgar, S., T.H.C. Herbers, M. Okihiro, J. Oltman-Shay, and R.T. Guza, Observations of infragravity waves, *J. Geophys. Res.*, *97*(C10), 15,573-15,577, 1992.

Guza, R.T., and E.B. Thornton, Swash oscillations on a natural beach, *J. Geophys. Res.*, *87*(C1), 483-491, 1982.

Guza, R.T., and E.B Thornton, Observations of surf beat, *J. Geophys. Res.*, *90*(C2), 3161-3172, 1985.

Guza, R.T., E.B. Thornton, and R.A. Holman, Swash on steep and shallow beaches, in *Proceedings of the 19th International Conference on Coastal Engineering*, edited by B.L. Edge, pp. 708-723, Am. Soc. of Civ. Eng., New York, 1984.

Herbers, T.H.C., S. Elgar, and R.T. Guza, Generation and propagation of infragravity waves, *J. Geophys. Res.*, *100*(C12), 24,863-24,872, 1995a.

Herbers, T.H.C., S. Elgar, R.T. Guza, and W.C. O'Reilly, Infragravity-frequency (0.005-0.05 Hz) motions on the shelf, II, Free waves, *J. Phys. Oceanogr.*, *25*(6), 1063-1079, 1995b.

Holland, K.T., B. Raubenheimer, R.T. Guza, and R.A. Holman, Runup kinematics on a natural beach, *J. Geophys. Res.*, *100*(C3), 4985-4993, 1995.

Holman, R.A., Infragravity energy in the surf zone, *J. Geophys. Res.*, *86*(C7), 6442-6450, 1981.

Holman, R.A., and A.J. Bowen, Bars, bumps, and holes: Models for the generation of complex beach topography, *J. Geophys. Res.*, *87*(C1), 457-468, 1982.

Holman, R.A., and A.H. Sallenger Jr , Setup and swash on a natural beach, *J. Geophys Res.*, *90*(C1), 945-953, 1985.

Holman, R.A , and A.H. Sallenger Jr., Sand bar generation: A discussion of the Duck experiment series, *J. Coastal Res.*, *SI*(15), 76-92, 1993.

Holman, R.A., P.A. Howd, J. Oltman-Shay, and P.D. Komar, Observations of the swash expression of far infragravity wave motions, in *Proceedings of the 22nd International Conference on Coastal Engineering*, edited by B.L. Edge, pp. 1242-1253, Am. Soc. of Civ. Eng., New York, 1990.

Howd, P.A., J. Oltman-Shay, and R.A. Holman, Wave variance partitioning in the trough of a barred beach, *J. Geophys. Res.*, *96*(C7), 12,781-12,795, 1991.

Howd, P.A., A.J. Bowen, and R.A. Holman, Edge waves in the presence of strong longshore currents, *J. Geophys. Res.*, *97*(C7), 11,357-11,371, 1992.

Huntley, D.A., Long-period waves on a natural beach, *J. Geophys. Res.*, *81*(36), 6441-6449, 1976.

Huntley, D.A., R.T. Guza, and A.J. Bowen, A universal form for shoreline run-up spectra?, *J. Geophys. Res.*, *82*(18), 2577-2581, 1977.

Huntley, D.A., R.T. Guza, and E.B. Thornton, Field observations of surf beat, 1, Progressive edge waves, *J. Geophys. Res.*, *86*(C7), 6451-6466, 1981.

Inman, D.L., and R.T. Guza, The origin of swash cusps on beaches, *Mar. Geol.*, *49*, 133-148, 1982.

Kobayashi, N., and E.A. Karjadi, Obliquely incident irregular waves in surf and swash zones, *J. Geophys. Res.*, *101*(C3), 6527-6542, 1996.

Longuet-Higgins, M.S., and R.W. Stewart, Radiation stresses in water waves; A physical discussion, with applications, *Deep Sea Res.*, *11*(4), 529-562, 1964.

Miche, R., Le pouvoir réfléchissant des ouvrages maritimes exposés à l'action de la houle, *Ann. Ponts Chaussées*, *121*, 285-319, 1951.

Okihiro, M., R.T. Guza, and R.J. Seymour, Bound infragravity waves, *J. Geophys. Res.*, *97*(C7), 11,453-11,469, 1992.

Oltman-Shay, J., and R.T. Guza, Infragravity edge wave observations on two California beaches, *J. Phys. Oceanogr.*, *17*(5), 644-663, 1987.

Oltman-Shay, J., and P.A. Howd, Edge waves on nonplanar bathymetry and alongshore currents: A model and data comparison, *J. Geophys. Res.*, *98*(C2), 2495-2507, 1993.

Oltman-Shay, J., P.A. Howd, and W.A. Birkemeier, Shear instabilities of the mean longshore current, 2, Field observations, *J. Geophys. Res.*, *94*(C12), 18,031-18,042, 1989.

Pawka, S., Island shadows in wave directional spectra, *J. Geophys. Res.*, *88*(C4), 2579-2591, 1983.

Pawka, S S., Wave directional characteristics on a partially sheltered coast, Ph.D. thesis, Scripps Inst. of Oceanogr., Univ. of Calif., San Diego, 1982.

Percival, D.B., and A.T. Walden, Spectral Analysis for Physical Applications: *Multitaper and Conventional Univariate Techniques*, 583 pp., Cambridge Univ. Press, New York, 1993.

Press, W.H., S.A Teukolsky, W.T. Vetterling, and B.P. Flannery, *Numerical Recipes in C: The Art of Scientific Computing*, 994 pp., Cambridge Univ. Press, New York, 1992

Raubenheimer, B., and R.T. Guza, Runup on a concave-shaped beach (abstract), *Eos Trans. AGU, 75(44)*, Fall Meet. Suppl., 321, 1994.

Raubenheimer, B., and R.T. Guza, Observations and predictions of run-up, *J. Geophys. Res* , *101*(C11), 25,575-25,587, 1996.

Raubenheimer, B., R.T. Guza, S. Elgar, and N. Kobayashi, Swash on a gently sloping beach, *J Geophys Res.*, *100*(C5), 8751-8760, 1995.

Suhayda, J.N., Standing waves on beaches, *J Geophys. Res.*, *79*(21), 3065-3071, 1974.

Ursell, F., Edge waves on a sloping beach, *Proc. R. Soc. London, Ser. A*, *214*, 79-97, 1952.

K. T. Holland, Naval Research Laboratory, Code 7442, Building 2438, Stennis Space Center, MS 39529. (tholland@nrlssc.navy.mil)

R. A. Holman, College of Oceanic and Atmospheric Sciences, Oregon State University, Corvallis, OR 97331.

(Received February 25, 1998; revised November 5, 1998, accepted February 17, 1999)